# Spatial Modulation-based Orthogonal Signal Division Multiplexing for Underwater ACOMMS

Zhuoran Qi and Dario Pompili
Department of Electrical and Computer Engineering, Rutgers University–New Brunswick, NJ, USA {zhuoran.qi, pompili}@rutgers.edu

Abstract—Orthogonal Signal Division Multiplexing (OSDM) has shown great robustness against multipath and Doppler effects in underwater acoustic channels, while however having a low spectral efficiency. In this work, a novel transmission method, named Spatial Modulation-based OSDM (SM-OSDM), is proposed to improve the spectral efficiency while keeping the Bit Error Rate (BER) low, where multiple transducers are utilized at the transmitter side but only one is active in each time slot. The simulation results prove that the SM-OSDM offers higher spectral efficiency than Single-Input Single-Output (SISO)-OSDM and lower BER compared with Multiple-Input Multiple-Output (MIMO)-OSDM.

Index Terms—Spatial modulation, orthogonal signal division multiplexing, underwater acoustic communication.

### I. Introduction

Underwater wireless communications play a vital role in the military, commercial, and scientific fields [1]. Some of its applications include natural resource and scientific ocean exploration, oceanic environment monitoring, communications between submarines and/or among Autonomous Underwater Vehicles (AUVs), and so on [2]. Due to the urgent demand for high transmission data rates over long-, medium- and shortrange distances (i.e., from hundreds of meters to kilometers), underwater Acoustic Communications (ACOMMS) are widely used [3]. Compared with Underwater Radio Frequency Communication (URFC) [4], [5] and Underwater Wireless Optical Communication (UWOC) [6], [7], underwater ACOMMS suffer from less attenuation and offer a longer coverage distance of several kilometers [8]. However, the acoustic wave speed is as slow as 1,500 m/s, leading to high latency; and the bandwidth of ACOMMS for medium/long ranges is limited and results in low transmission data rates [9], [10]. Moreover, the underwater acoustic channel is time varying and is affected by multipath [11], especially in shallow water (depth less than 100 m). Even though the transmitter and receiver are fixed, the water wave is dynamic and causes Doppler frequency shifts. Therefore, a transmission method that is able to improve the transmission data rate as well as is robust against multipath and Doppler effects for underwater ACOMMS is in great need.

**Existing Works:** In [12], an underwater transceiver structure is proposed with the Pulse Position Modulation (PPM)-based Orthogonal Frequency Division Multiplexing (OFDM), which only works for UWOC with low latency and few multipath delays. In [13], a nonlinear and non-coherent modulation scheme, called Circular Time Shift Modulation (CTSM), is proposed to transmit signals in high multipath delay and high

noise underwater channels; however, the spectral efficiency of CTSM is very low. Authors in [14] conduct experiments with Spatial Modulation (SM) in underwater acoustic channels and demonstrate that SM increases bandwidth and power efficiency compared to temporal modulation. Authors in [15] study the performance of the SM-based Multiple-Input Multiple-Output (MIMO) system in fading channels, which shows high robustness. In [16], the OFDM is applied to underwater ACOMMS. The spectral efficiency is improved by OFDM, but OFDM leads to a high Peak-to-Average Power Ratio (PAPR) and can result in distortions in linear devices (e.g., amplifiers). Authors in [17] propose a new method of information transmission as an alternative to OFDM, called Orthogonal Signal-Division Multiplexing (OSDM), which achieves lower PAPR and higher robustness against the Doppler effect. The OSDM is also proved to be efficient in the underwater environment with doubly spread channels and impulsive noise [18]. To improve the transmission data rate, the authors in [19] propose a MIMO-OSDM, where the transmission data rate is improved by spatial multiplexing; however, the interference between different data streams increases the Bit Error Rate (BER).

Contributions: In this work, we propose a novel transmission scheme called SM-OSDM. In SM, a block of information bits is mapped to a source-coded symbol at a certain transmit antenna, and only this antenna is active at the time slot, while the other antennas do not transmit symbols. The transceiver structure of the SM-OSDM is designed, and the modulation/demodulation process is demonstrated. The equations of modulator/demodulator are derived. The physicallayer evaluation of the SM-OSDM system is carried out based on MATLAB simulations in a realistic underwater acoustic channels with different water wave speeds (the moving speeds of the propagation medium) and varying Signal-to-Noise Ratio (SNR) values. The BER and spectral efficiency of the proposed SM-OSDM are evaluated and compared with ordinary Single-Input Single-Output (SISO)-OSDM and MIMO-OSDM in different scenarios. The simulation results show that the SM-OSDM achieves a higher spectral efficiency than SISO-OSDM and a lower BER than MIMO-OSDM with multipath and Doppler effects.

**Paper Organization:** In Sect. II, we present the system structure of our proposed SM-OSDM. In Sect. III, we discuss the simulation results of SM-OSDM in realistic channels. Finally, we draw our conclusions in Sect. IV.

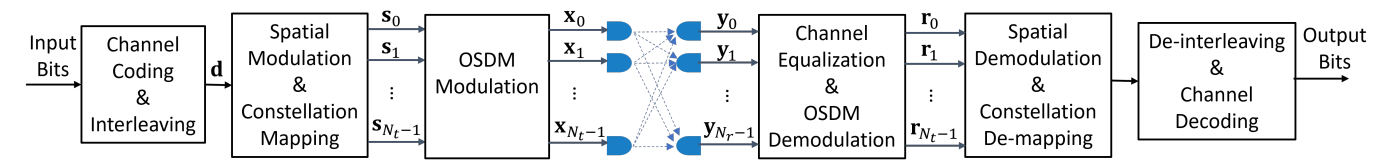


Fig. 1: High-level structure of our custom-made physical-layer simulator, including both the transmitter and the receiver.

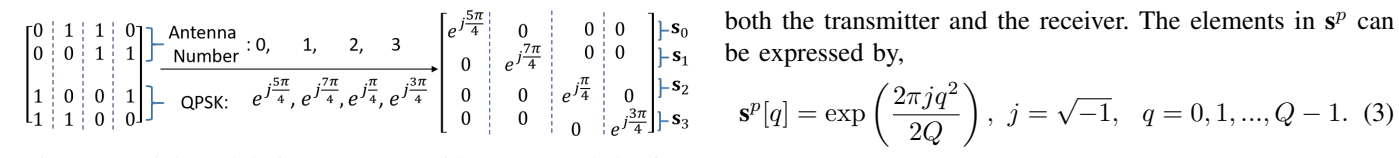


Fig. 2: Spatial modulation structure with QPSK and the four trasducers. Gray code is applied  $(i = \sqrt{-1})$ .

## II. PROPOSED SPATIAL MODULATION OSDM

To improve the spectral efficiency and reduce the interference between data streams, we propose a novel transmission scheme called SM-OSDM by applying SM to OSDM transmissions. The system structure is shown in Fig. 1. At the transmitter side, the channel coding and interleaving are first applied to the input bit sequence. Then the coded bits are modulated with spatial modulation and constellation symbols are placed to generate different symbol streams for different transducers. After the OSDM modulation, the SM-OSDM signals for different trasducers are transmitted. At the receiver, the channels are estimated by analyzing the pilot sequences. After channel equalization and OSDM demodulation, the spatial demodulation and constellation de-mapping is done to get the demodulated bits. Finally, the output bits are obtained by de-interleaving and performing channel decoding.

**Transmitter:** Given a sequence of channel coded bits **d**, assume the length of **d** is  $M_d$ . The number of transducers at the trasmitter is  $N_t$ . The source coding scheme is M-ary Phase Shift Keying (PSK). In SM, first, the coded bits **d** is divided into N blocks, each block containing K bits,  $M_d = NK$ ,  $K = \log_2 N_t + \log_2 M$ . For instance, as shown in Fig. 2, 16 bits are divided into 4 blocks, each block containing 4 bits. The number of transducers is  $N_t = 4$  and Quadrature PSK (QPSK, M=4) is applied. Therefore, in each block, the first  $\log_2 N_t = 2$  bits decide which transducers is active, and the last  $\log_2 M = 2$  bits are modulated into QPSK symbol.

Let  $\mathbf{s}_{n_t}$  represents the SM-modulated signal at each transducer,  $n_t = 0, 1, ..., N_t - 1$ ,

$$\mathbf{s}_{n_t} = [s_{n_t,0} \ s_{n_t,1} \ \dots \ s_{n_t,N-1}]. \tag{1}$$

To modulate each SM signal with OSDM,  $\mathbf{s}_{n_t}$  is divided to P blocks. Each block  $\mathbf{m}_{n_t,p}$  has a length of Q, p =0, 1, ..., P - 1, N = PQ

$$\mathbf{s}_{n_t} = [\mathbf{m}_{n_t,0} \ \mathbf{m}_{n_t,1} \ \dots \ \mathbf{m}_{n_t,P-1}].$$
 (2)

To estimate the channel, the high-autocorrelation common pilot sequence  $\mathbf{s}^p$  is created with a length of Q, shared by

$$\mathbf{s}^{p}[q] = \exp\left(\frac{2\pi j q^{2}}{2Q}\right), \ j = \sqrt{-1}, \ q = 0, 1, ..., Q - 1.$$
 (3)

Based on the common pilot sequence, the pilot sequence for each transducer is given by,

$$\mathbf{s}_{n_t}^p = \mathbf{s}^p(\mathbf{Z}_Q)^{n_t \hat{Q}}, \quad \hat{Q} = \lfloor Q/N_t \rfloor, \tag{4}$$

where "| · |" denotes the nearest integer in the direction of negative infinity.  $\mathbf{Z}_Q$  is the cyclic shift matrix of size  $Q \times Q$ ,

$$\mathbf{Z}_{Q} = \begin{bmatrix} 0 & 1 & 0 & \cdots & 0 \\ 0 & 0 & 1 & \cdots & 0 \\ \vdots & \vdots & \vdots & \ddots & 0 \\ 0 & 0 & 0 & \cdots & 1 \\ 1 & 0 & 0 & \cdots & 0 \end{bmatrix}.$$
 (5)

After adding the pilot sequences in front of each SM signal, the symbol vector  $\mathbf{c}_{n_t}$  with the length of JQ is created, J =

$$\mathbf{c}_{n_{t}} = [\mathbf{s}_{n_{t}}^{p} \ \mathbf{m}_{n_{t},0} \ \mathbf{m}_{n_{t},1} \ \dots \ \mathbf{m}_{n_{t},P-1}].$$
 (6)

Based on OSDM modulation, the transmitted signal at each transducer is,

$$\mathbf{x}_{n_t} = \mathbf{c}_{n_t}(\mathbf{F}_J \otimes \mathbf{I}_Q),\tag{7}$$

where " $\otimes$ " denotes the Kronecker product,  $I_Q$  is the identity matrix of size  $Q \times Q$ ,  $\mathbf{F}_J$  is the Inverse Discrete Fourier Transform (IDFT) [20] matrix of size  $J \times J$ ,

$$\mathbf{F}_{J} = \frac{1}{\sqrt{J}} \begin{bmatrix} W_{J}^{0} & W_{J}^{0} & \cdots & W_{J}^{0} \\ W_{J}^{0} & W_{J}^{1} & \cdots & W_{J}^{J-1} \\ \vdots & \vdots & \ddots & \vdots \\ W_{J}^{0} & W_{J}^{J-1} & \cdots & W_{J}^{(J-1)^{2}} \end{bmatrix},$$
(8)  
$$W_{J}^{k} = \exp\left(\frac{2\pi jk}{J}\right), \ j = \sqrt{-1}.$$

In this way, the pilot and data sequences are arranged on a rectangular lattice in the time-frequency domain and do not interfere with each other.

**Receiver:** Assume there are  $N_r$  hydrophones at the receiver,  $N_r \geq N_t$ . The channel response at the link  $(n_t, n_r)$  is,

$$\mathbf{h}^{(n_t, n_r)} = [h_0^{(n_t, n_r)} \ h_1^{(n_t, n_r)} \ \dots]. \tag{9}$$

The received signal at the  $n_r$ -th hydrophone is,

$$\hat{\mathbf{y}}_{n_r} = \sum_{n_t=0}^{N_t-1} \mathbf{x}_{n_t} * \mathbf{h}^{(n_t, n_r)} + \boldsymbol{\eta}_{n_r},$$
 (10)

where  $n_r = 0, 1, ..., N_r - 1$ , "\*" denotes the convolution operation, and  $\eta_{n_r}$  is the additive noise at the  $n_r$ -th hydrophone.

To reduce the Inter-Symbol Interference (ISI), a Cyclic Prefix (CP) with a length of L is added, with  $L \leq Q$ . Assume  $L_t$  is the maximum multipath delay in the time-discrete model. When  $L \geq L_t$ , the channel reverberation is correctable. The CP-removed sequence  $\mathbf{y}_{n_r}$  can be expressed by,

$$\mathbf{y}_{n_r} = \sum_{n_t=0}^{N_t-1} \mathbf{x}_{n_t} \mathbf{H}^{(n_t, n_r)} + \boldsymbol{\eta}_{n_r},$$

$$\mathbf{H}^{(n_t, n_r)} = \begin{bmatrix} h_0^{(n_t, n_r)} & h_1^{(n_t, n_r)} & \cdots & h_{JQ-1}^{(n_t, n_r)} \\ h_{JQ-1}^{(n_t, n_r)} & h_0^{(n_t, n_r)} & \cdots & h_{JQ-2}^{(n_t, n_r)} \\ \vdots & \vdots & \ddots & \vdots \\ h_1^{(n_t, n_r)} & h_2^{(n_t, n_r)} & \cdots & h_0^{(n_t, n_r)} \end{bmatrix}.$$
(11)

To demodulate the OSDM signals, the transformed received signal vector **z** is created based on (7) and (11),

$$\mathbf{z} = [\mathbf{y}_0 \quad \mathbf{y}_1 \quad \dots \quad \mathbf{y}_{N_r}] (\mathbf{I}_{N_r} \otimes \mathbf{F}_J^H \otimes \mathbf{I}_Q)$$

$$= [\mathbf{c}_0 \quad \mathbf{c}_1 \quad \dots \quad \mathbf{c}_{N_t-1}] \mathbb{H}_{comb} + \hat{\boldsymbol{\eta}}$$

$$= [\mathbf{z}_0 \quad \mathbf{z}_1 \quad \dots \quad \mathbf{z}_{N_r-1}] + \hat{\boldsymbol{\eta}},$$
(12)

where  $[\cdot]^H$  denotes the conjugate matrix and  $\hat{oldsymbol{\eta}}$  is the transformed additive noise. The combined channel matrix is,

$$\mathbb{H}_{comb} = \begin{bmatrix} \mathbb{H}^{(0,0)} & \mathbb{H}^{(0,1)} & \dots & \mathbb{H}^{(0,N_r-1)} \\ \mathbb{H}^{(1,0)} & \mathbb{H}^{(1,1)} & \dots & \mathbb{H}^{(1,N_r-1)} \\ \vdots & \vdots & \ddots & \vdots \\ \mathbb{H}^{(N_t-1,0)} & \mathbb{H}^{(N_t-1,1)} & \dots & \mathbb{H}^{(N_t-1,N_r-1)} \end{bmatrix}.$$
(13)

 $\mathbb{H}^{(n_t,n_r)}$  is the multipath delay channel matrix,

$$\mathbb{H}^{(n_t, n_r)} = \operatorname{diag}(\mathbb{H}_0^{(n_t, n_r)}, \ \mathbb{H}_1^{(n_t, n_r)}, \ ..., \ \mathbb{H}_{J-1}^{(n_t, n_r)}),$$
 (14)

where  $\mathrm{diag}(\cdot)$  represents the block diagonal matrix. The submatrix  $\mathbb{H}_k^{(n_t,n_r)}$  is defined by,

$$\mathbb{H}_{k}^{(n_{t},n_{r})} = \begin{bmatrix} h_{0}^{(n_{t},n_{r})} & h_{1}^{(n_{t},n_{r})} & \cdots & h_{Q-1}^{(n_{t},n_{r})} \\ W_{J}^{-k}h_{Q-1}^{(n_{t},n_{r})} & h_{0}^{(n_{t},n_{r})} & \cdots & h_{Q-2}^{(n_{t},n_{r})} \\ \vdots & \vdots & \ddots & \vdots \\ W_{J}^{-k}h_{1}^{(n_{t},n_{r})} & W_{J}^{-k}h_{2}^{(n_{t},n_{r})} & \cdots & h_{0}^{(n_{t},n_{r})} \end{bmatrix}.$$

The elements in (12) are calculated by,

$$\begin{split} \mathbf{z}_{n_r} &= \sum_{n_t=0}^{N_t-1} \mathbf{c}_{n_t} \mathbb{H}^{(n_t,n_r)} \\ &= \sum_{n_t=0}^{N_t-1} [\mathbf{s}_{n_t}^p \ \mathbf{m}_{n_t,0} \ \mathbf{m}_{n_t,1} \ \dots \ \mathbf{m}_{n_t,P-1}] \mathbb{H}^{(n_t,n_r)} \\ &= [\mathbf{z}_{n_r}^p \ \mathbf{z}_{n_r,0} \ \mathbf{z}_{n_r,1} \ \dots \ \mathbf{z}_{n_r,P-1}], n_r = 0, 1, ..., N_r - 1. \end{split}$$

Therefore, the received pilot sequence at the  $n_r$ -th receiver is,

$$\mathbf{z}_{n_r}^p = \sum_{n_t=0}^{N_t-1} \mathbf{s}_{n_t}^p \mathbb{H}_0^{(n_t, n_r)} = \mathbf{s}^p \sum_{n_t=0}^{N_t-1} (\mathbf{Z}_Q)^{n_t \hat{Q}} \mathbb{H}_0^{(n_t, n_r)}.$$
(17)

Now, if we assume  $\hat{Q} \geq L_t$ ,

$$\mathbf{h}^{(n_t,n_r)} = [h_0^{(n_t,n_r)} \ h_1^{(n_t,n_r)} \ \dots \ h_{\hat{Q}}^{(n_t,n_r)} \ \mathbf{0}_{1\times(Q-\hat{Q})}], \ (18)$$

$$\hat{\mathbf{h}}^{(n_t, n_r)} = [h_0^{(n_t, n_r)} \ h_1^{(n_t, n_r)} \ \dots \ h_{\hat{Q}}^{(n_t, n_r)}], \quad (19)$$

where  $\mathbf{0}_{1 \times (Q - \hat{Q})}$  is the zero matrix of size  $1 \times (Q - \hat{Q})$ . Let  $\mathbb{H}_0^{n_r} = \sum_{n_t=0}^{N_t-1} (\mathbf{Z}_Q)^{n_t\hat{Q}} \mathbb{H}_0^{(n_t,n_r)}$ , which can be calculated by  $\mathbb{H}_0^{n_r} = (\mathbf{s}^p)^H \mathbf{z}_{n_r}^p / ||\mathbf{s}^p||^2$  according to (17). Then the channel response can be estimated as,

$$\mathbb{H}_0^{n_r} \mathbf{I}_{1 \times Q} = [\hat{\mathbf{h}}^{(0,n_r)} \ \hat{\mathbf{h}}^{(1,n_r)} \ \dots \ \hat{\mathbf{h}}^{(N_t-1,n_r)} \ \mathbf{0}_{1 \times (Q-\hat{Q})}], \tag{20}$$

where  $\mathbf{I}_{1\times Q} = \begin{bmatrix} 1 & 0 & 0 & \dots & 0 \end{bmatrix}$ .

Given the estimated combined channel matrix  $\hat{\mathbb{H}}_{comb}$ , the channel equalized signals are calculated by,

$$[\mathbf{r}_0 \ \mathbf{r}_1 \ \dots \ \mathbf{r}_{N_t-1}] = \mathbf{z} \hat{\mathbb{H}}_{comb}^H (\hat{\mathbb{H}}_{comb} \hat{\mathbb{H}}_{comb}^H)^{-1}, \tag{21}$$

where  $[\cdot]^{-1}$  denotes the inverse matrix.

$$\hat{\mathbb{H}}_{comb} = \begin{bmatrix} \hat{\mathbb{H}}^{(0,0)} & \hat{\mathbb{H}}^{(0,1)} & \dots & \hat{\mathbb{H}}^{(0,N_r-1)} \\ \hat{\mathbb{H}}^{(1,0)} & \hat{\mathbb{H}}^{(1,1)} & \dots & \hat{\mathbb{H}}^{(1,N_r-1)} \\ \vdots & \vdots & \ddots & \vdots \\ \hat{\mathbb{H}}^{(N_t-1,0)} & \hat{\mathbb{H}}^{(N_t-1,1)} & \dots & \hat{\mathbb{H}}^{(N_t-1,N_r-1)} \end{bmatrix},$$

$$\hat{\mathbb{H}}^{(n_t,n_r)} = \operatorname{diag}(\mathbb{H}_1^{(n_t,n_r)}, \mathbb{H}_2^{(n_t,n_r)}, \dots, \mathbb{H}_P^{(n_t,n_r)}).$$
(22)

Spatial demodulation is performed by analyzing the maximum power of symbols at the different hydrophones in each

time slot, while the constellation de-mapping is done based on the minimal Euclidean distance. The demodulated bits are de-interleaved and channel decoded to obtain the output bits.

# III. PERFORMANCE EVALUATION

We now describe the physical-layer simulator of our proposed SM-OSDM system and introduce its parameters in detail. The turbo coding with the coding rate of  $R_{ch} = 1/3$ is utilized to enhance the system reliability. The coded bits are modulated by QPSK in SM. The simulation channels are assumed to be Rayleigh fading with multipath delay and Doppler effects. The symbol rate is  $R_s = 6$  kBd. The frequency band is 8 kHz - 14 kHz and the bandwidth is  $B_w = 6 \text{ kHz}$ . The sampling frequency is 9.6 kHz. The carrier frequency is 11 kHz. The transmitter and the receiver are assumed to be static, while the water wave speed is assumed to be 0-0.3 m/s. Furthermore, J=4, P=64, and L=16. The maximum multipath delay is 1.67 ms.

In Fig. 3, the BER versus normalized SNR (Eb/No) with different water wave speeds is depicted. We can observe that the BER performance of 4-by-4 SM-OSDM is better than 4-by-4 MIMO-OSDM, since only one transducer is active to transmit interest information in each time slot for SM-OSDM, and there is less interference between different streams. Nonetheless, the BER of SM-OSDM is worse than SM-SISO, because inactive transducers in each time slot still transmit pilot sequences for channel estimation and the identification of the active transducer at the receiver, which

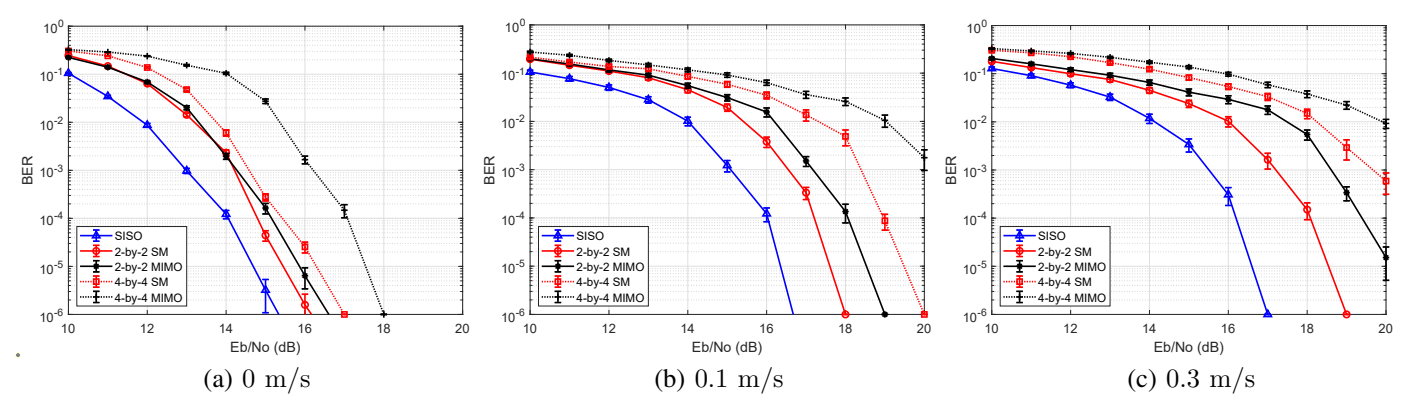


Fig. 3: The Bit Error Rate (BER) versus normalized SNR (Eb/No) with different modulation schemes when the water wave speed is (a) 0 m/s; (b) 0.1 m/s; (c) 0.3 m/s. The 95% confidence intervals are depicted.

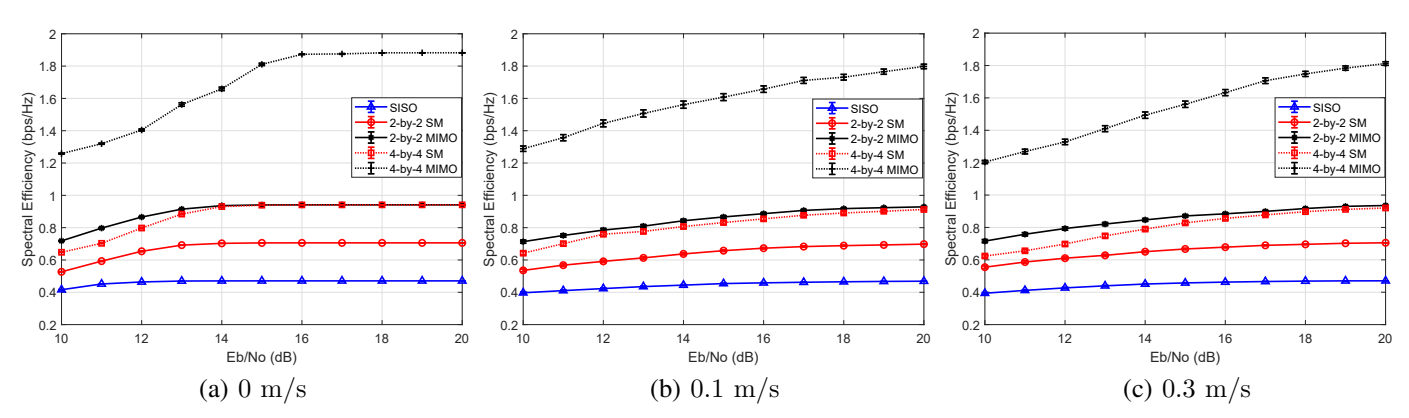


Fig. 4: The spectral efficiency versus Eb/No with different modulation schemes when the water wave speed is (a) 0 m/s; (b) 0.1 m/s; (c) 0.3 m/s. The 95% confidence intervals are less than  $10^{-2}$  and hence are not visible in the figures.

results in interference. We can also observe that the BER of the 4-by-4 SM-OSDM is higher than for the 2-by-2 SM-OSDM, because the 4-by-4 system suffers from higher interference between transducers. As shown in Fig. 3(a), where the water wave speed is 0 m/s, the BER of the 2-by-2 SM-OSDM is close to that of the 2-by-2 MIMO-OSDM, but in Figs. 3(b) and (c) it is obvious that the BER of the 2-by-2 SM-OSDM is better than that of the 2-by-2 MIMO-OSDM, since the SM-OSDM provides higher robustness against the Doppler effects. In Fig. 4, the spectral efficiency is calculated by

In Fig. 4, the spectral efficiency is calculated by  $\frac{R_sNKR_{ch}}{B_w(N+L)}(1-\text{BER})$ . It can be observed that the 4-by-4 MIMO-OSDM provides the highest spectral efficiency, but its efficiency decreases dramatically when the SNR is lower than 16 dB. The 2-by-2 MIMO-OSDM is close to the 4-by-4 SM-OSDM and is better when the SNR is low and the Doppler is high. Therefore, as expected, we can conclude that there is a trade-off between BER and spectral efficiency: when a low BER is needed, the 2-by-2 SM-OSDM should be used; on the other hand, when achieving a high spectral efficiency is more important, the 4-by-4 MIMO-OSDM should be adopted.

## IV. CONCLUSION AND FUTURE WORK

We proposed a novel physical-layer transmission scheme for underwater ACOMMS, called SM-OSDM. We conducted a series of simulations to evaluate its performance. The results showed that the SM-OSDM achieved a lower BER than MIMO-OSDM with the same deployment of transducers and hydrophones, especially in high Doppler channels. The SM-OSDM also offered a higher spectral efficiency than SISO-OSDM. The trade-off between BER and spectral efficiency was discussed as well.

As future work, we will conduct testbed-based underwater ACOMMS experiments with different combinations of J and P values. New pilot sequence structures will be explored for the SM-OSDM systems to improve the robustness against multipath and Doppler effects. The SM-OSDM will be further extended by utilizing massive MIMO deployments. The performance of SM-OSDM with different underwater vehicle speeds will be presented.

**Acknowledgement:** We thank Rutgers Ph.D. student Biswajit Kumar Dash for helping out with the study. This work was supported by NSF NeTS Award No. CNS-1763964.

### REFERENCES

- M. Ali, D. N. Jayakody, T. Perera, A. Sharma, K. Srinivasan, and I. Krikidis, "Underwater communications: Recent advances," in *International Conference on Emerging Technologies of Information and Communications (ETIC)*, 2019, pp. 1–10.
- [2] M. Rahmati, A. Gurney, and D. Pompili, "Adaptive underwater video transmission via software-defined MIMO acoustic modems," in OCEANS 2018 MTS/IEEE Charleston, 2018, pp. 1–6.
- [3] M. Zia, J. Poncela, and P. Otero, "State-of-the-art underwater acoustic communication modems: Classifications, analyses and design challenges," in Wireless Personal Communications, 2021, pp. 1325–1360.
- [4] M. Soomro, S. N. Azar, O. Gurbuz, and A. Onat, "Work-in-progress: Networked control of autonomous underwater vehicles with acoustic and radio frequency hybrid communication," in *IEEE Real-Time Systems Symposium (RTSS)*, 2017, pp. 366–368.
- [5] M. Rauf, M. Aamir, and A. M. Khan, "A prospect of efficient radio-frequency based underwater wireless data transfer," in 2020 Global Conference on Wireless and Optical Technologies (GCWOT), 2020, pp. 1-5.
- [6] M. Doniec, M. Angermann, and D. Rus, "An end-to-end signal strength model for underwater optical communications," *IEEE Journal* of Oceanic Engineering, vol. 38, no. 4, pp. 743–757, Oct 2013.
- [7] H. Kaushal and G. Kaddoum, "Underwater optical wireless communication," in *IEEE Access*, vol. 4, 2016, pp. 1518–1547.
- [8] A. Rodionov, S. Kulik, F. Dubrovin, and P. Unru, "Experimental estimation of the ranging accuracy using underwater acoustic modems in the frequency band of 12 kHz," in *The 27th Saint Petersburg International Conference on Integrated Navigation Systems (ICINS)*, 2020, pp. 1–3.
- [9] M. Stojanovic, "On the relationship between capacity and distance in an underwater acoustic communication channel," in *Proceedings of the* ACM International Workshop on Underwater Networks, Sep 2006, pp. 41–47.
- [10] D. Pompili and I. F. Akyildiz, "A multimedia cross-layer protocol for underwater acoustic sensor networks," *IEEE Transactions on Wireless Communications*, vol. 9, no. 9, pp. 2924–2933, 2010.

- [11] D. Pompili, T. Melodia, and I. F. Akyildiz, "Three-dimensional and two-dimensional deployment analysis for underwater acoustic sensor networks," in *Ad Hoc Networks*, vol. 7, no. 4, 2009, pp. 778 – 790.
- [12] Z. Qi, X. Zhao, and D. Pompili, "Range-extending optical transceiver structure for underwater vehicles and robotics," in *Proceedings of the International Conference on Underwater Networks & Document Systems*, ser. WUWNET'19. New York, NY, USA: Association for Computing Machinery, 2019.
- [13] Z. Qi and D. Pompili, "UW-CTSM: Circular time shift modulation for underwater acoustic communications," in 17th Wireless On-Demand Network Systems and Services Conference (WONS), 2022, pp. 1–8.
- [14] D. Kilfoyle, J. Preisig, and A. Baggeroer, "Spatial modulation experiments in the underwater acoustic channel," *IEEE Journal of Oceanic Engineering*, vol. 30, no. 2, pp. 406–415, 2005.
- [15] S. S. Pillai, S. Dhanya, and B. K. Jeemon, "Performance comparison of multicast MIMO systems employing spatial modulation and coded spatial modulation in fading channels," in *International Conference* on *Intelligent Computing, Instrumentation and Control Technologies* (ICICICT), 2017, pp. 1529–1533.
- [16] M. Rahmati, Z. Qi, and D. Pompili, "Underwater adaptive video transmissions using MIMO-based software-defined acoustic modems," in *IEEE Transactions on Multimedia*, 2021, pp. 1–13.
- [17] A. Mahmood and M. Chitre, "Detecting OSDM signals in sparse channels and snapping shrimp noise," in *The 4th Underwater Commu*nications and Networking Conference (UComms), 2018, pp. 1–5.
- [18] T. Ebihara and K. Mizutani, "Underwater acoustic communication with an orthogonal signal division multiplexing scheme in doubly spread channels," in *IEEE Journal of Oceanic Engineering*, vol. 39, no. 1, 2014, pp. 47–58.
- [19] T. Ebihara, H. Ogasawara, and G. Leus, "Underwater acoustic communication using multiple-input-multiple-output doppler-resilient orthogonal signal division multiplexing," in *IEEE Journal of Oceanic Engineering*, vol. 45, no. 4, 2020, pp. 1594–1610.
- [20] N. Suehiro, R. Jin, C. Han, and T. Hashimoto, "Performance of very efficient wireless frequency usage system using kronecker product with rows of DFT matrix," in 2006 IEEE Information Theory Workshop -ITW '06 Chengdu, 2006, pp. 526–529.